

Impaired Proliferation and Migration in Human Miller-Dieker Neural Precursors

Volney L. Sheen,¹ MD, PhD, Russell J. Ferland,¹ PhD, Megan Harney,¹ BA, R. Sean Hill,¹ PhD, Jason Neal,¹ BA, Alison H. Banham,² MA, DPhil, Philip Brown,² BSc, DPhil, Anjen Chenn,³ MD, PhD, Joseph Corbo,⁴ MD, PhD, Jonathan Hecht,⁵ MD, Rebecca Folkerth,⁴ MD, and Christopher A. Walsh,^{1,6} MD, PhD

Objective: Miller-Dieker syndrome (MDS) is a malformation of cortical development that results in lissencephaly (meaning smooth brain). This disorder is caused by heterozygous deletions on chromosome 17p13.3, including the *lissencephaly 1 (LIS1)* gene. Various mouse models have been used as an experimental paradigm in understanding human lissencephaly, but clear limitations exist in these studies, particularly because mice are naturally lissencephalic. Thus, the objective of this article was to establish human neural precursor cell lines from postmortem MDS tissue and to characterize the pathological cellular processes that contribute to the human lissencephalic phenotype.

Methods: Human neural precursors were isolated and expanded from the frontal cortices of a 33-week postmortem fetus with MDS and an age-matched control subject. Relative rates of proliferation and cell death were assessed in vitro, whereas the migration of precursors was examined after transplantation in vivo.

Results: Precursors showed haploinsufficiency of the *LIS1* gene and a reduction in LIS1 protein. Precursors could also differentiate into both neurons and glia. MDS precursors demonstrated impairments in neuronal migration, diminished rates of cell proliferation, and increased cell death.

Interpretation: These results suggest that, in addition to migration, disruption in cell proliferation could play a more important role in the development of lissencephaly than previously suspected.

Ann Neurol 2006;60:137–144

Disorders of the human cerebral cortex arise from disruptions of genes involved in the normal cellular and molecular mechanisms that guide cortical development. Although many of the genes for these disorders recently have been identified, the pathophysiological mechanisms causing these malformations of cortical development are not entirely understood. For instance, classical lissencephaly (meaning smooth brain, OMIM 607432) is caused by mutations in the *lissencephaly 1 (LIS1)* gene. The more severe form of lissencephaly seen in Miller-Dieker syndrome (MDS) results from deletions along chromosome 17p13.3 and uniformly involves loss of function in a subset of genes including *LIS1* and *YWHAE*.^{1–4} Disruptions in these genes lead to altered microtubule dynamics^{5,6} and defects in neuronal migration in mice.^{7,8} However, unlike humans with MDS, in whom the cortex is lissencephalic and

highly disrupted and lateral ventricles are enlarged due to a heterozygous *LIS1* mutation, heterozygous *Lis1* mice display only mild cortical disorganization resulting from delayed neuronal migration.⁷ These observations are confounded by that normal mice are naturally lissencephalic and have no sulci or gyri. Thus, to what extent impairments in neural precursor migration and other developmental processes due to MDS deletions in humans, as opposed to other species, contribute to lissencephaly has not been fully explored.

Subject and Methods

Ethical and Licensing Considerations for Human Tissue

The following proposed studies have been approved by the Institutional Review Board at the Beth Israel Deaconess Medical Center and Brigham and Women's Hospital. De-

From the ¹Department of Neurology, Division of Neurogenetics and Howard Hughes Medical Institute, Beth Israel Deaconess Medical Center, Harvard Medical School, Boston, MA; ²Nuffield Department of Clinical Laboratory Sciences, University of Oxford, Level 4 Academic Block, John Radcliffe Hospital, Oxford, Oxfordshire, OX3 9DU, UK, United Kingdom; ³Department of Pathology, Northwestern University, Feinberg School of Medicine, Chicago, IL; ⁴Department of Neuropathology, Brigham and Women's Hospital, Harvard Medical School; ⁵Department of Neuropathology, Beth Israel Deaconess Medical Center, Harvard Medical School; and ⁶Program in Biological and Biomedical Sciences, Harvard Medical School, Boston, MA.

Received Nov 11, 2005, and in revised form Jan 23, 2006. Accepted for publication Feb 25, 2006.

Published online Apr 26, 2006 in Wiley InterScience (www.interscience.wiley.com). DOI: 10.1002/ana.20843

Address correspondence to Dr Sheen, Division of Neurogenetics and Howard Hughes Medical Institute, Department of Neurology, Beth Israel Deaconess Medical Center, Harvard Medical School, Boston, MA 02115. E-mail: vsheen@bidmc.harvard.edu

identified human tissue was obtained from pathological samples, available during autopsy and postmortem study. The diagnosis of the MDS neurological disorder was made before autopsy by prenatal genetic testing with fluorescent in situ hybridization. The fetus had an abnormal high-resolution karyotype with partial trisomy of 1p (<400 bands) and partial monosomy of 17p. A control age-matched postmortem brain was obtained for comparison and processed in an identical manner. All studies were performed with early passage (<10) cultures to minimize possibility of cell transformations over time. Affymetrix (Affymetrix, Santa Clara, CA) gene profiling of different neurosphere lines showed fair uniformity between neurospheres (data not shown).

Tissue Dissociation and Isolation

Methods for ventricular zone dissection and dissociation follow general guidelines used previously in murine cortical cell dissociations.^{9,10} In brief, the brains were cut into coronal sections; the samples were dissected to obtain tissue along the periventricular zone within the frontal cortex, minced and washed in cold Hanks buffered saline solution, and placed in trypsin solution at 37°C for 30 minutes. The samples were then passed through a cell strainer to isolate single cells and washed in Dulbecco's modified eagle medium (GIBCO, Burlington, Ontario, Canada) with 10% fetal calf serum to inactivate the trypsin. The dissociated cells were spun down, the media were aspirated, and the cells were placed in neurosphere medium (Cambrex bullet kit; Cambrex, East Rutherford, NJ) containing epidermal growth factor, fibroblast growth factor, neural cell survival factor, gentamycin, and amphotericin B for expansion. The cultures were maintained in a 37°C/5% CO₂ incubator, and media were aspirated and renewed on a weekly basis. Individual neurospheres were dissociated and reexpanded to ensure a clonal population.

Genetic Analysis

Cytogenetic analysis of the expanded neural precursor population can be performed using standard fluorescent in situ hybridization techniques.¹¹ Labeling of the BAC (bacterial artificial chromosomes) probes followed standard procedures with deoxyuridine triphosphate containing rhodamine and fluorescein tags (methods outlined in the Vysis nick translation kit; Vysis, Grove, IL). Hybridization was performed by denaturing the slides in 70% formamide/2×SSC (sodium chloride sodium citrate), dehydrating the slides with serial ethanol washes, and applying the probe to the slide samples. After hybridization, the slides were washed, coverslipped, and examined under fluorescence microscopy (Zeiss Axioskop; Zeiss, Thornwood, NY). Finally, routine karyotyping was performed on the cell lines (Boston University School of Medicine, Center for Human Genetics, Boston, MA).

The chromosomal region containing the deletion was screened using the following fluorescently labeled human MapPairs: *D17s1849*, *D17s1840*, *D17s1529*, *D17s1533*, *D17s1828*, *D17s1876*, and *D17S938*. Polymerase chain reaction products using these primers were analyzed on an ABI Prism 3100 (Applied Biosystems, Foster City, CA). Allele sizes were determined using Genotyper 3.7 (Applied Biosystems). The maximal deletion region was determined by loss of heterozygosity mapping.

Western Blot Analysis

Protein was extracted from the neural precursors by slight modifications of previously described methods,¹² solubilized in lysis buffer, separated on 7.5% sodium dodecyl sulfate polyacrylamide gel electrophoresis, and transferred onto polyvinylidene difluoride membrane. Membranes were probed with anti-nestin and anti-vimentin antibodies and detected by enhanced chemiluminescence. Antibodies for nestin (RD Systems, Minneapolis, MN) and vimentin (Zymed Laboratory, San Francisco, CA) were obtained commercially.

Immunocytochemistry

The neural precursors were plated onto glass slide chambers coated with poly-D-lysine (Becton Dickinson, San Jose, CA) for several hours and fixed with 4% paraformaldehyde in phosphate-buffered saline (PBS) or -80°C methanol. The cultures were placed in blocking solution with PBS containing 10% fetal calf serum, 5% horse serum, and 5% goat serum or 10% donkey serum; incubated overnight in the appropriate antibody (vimentin: stock [Zymed]; nestin: 5µg/ml [R&D Systems]; phospho-histone H3: 1:200 dilution of stock [Upstate Biotechnology, Lake Placid, NY]; α-/β-catenin: 1:250 dilution of stock [BD Transduction Laboratories, San Jose, CA]); and processed through standard fluorescent secondary antibodies (CY3 [Jackson Immunoresearch Laboratories, West Grove, PA] and fluorescein isothiocyanate [Sigma, St. Louis, MO]).

Electron Microscopy

Processing of neurospheres for electron microscopy followed previously published methods.^{13,14} In brief, the cell suspensions were fixed in EM fixative (4% sucrose, 2.5% glutaraldehyde, and 2% paraformaldehyde in piperazine diethanesulfonic acid buffer). Cells were spun down, and supernatant was replaced with 0.1M PBS. Pellets were osmicated with 1% osmium tetroxide, washed with PBS, and washed with distilled water. Pellets then were placed in 1% uranyl acetate at room temperature, washed in distilled water, and serially dehydrated in ethanol. One milliliter of propylene oxide was placed in each sample and then replaced with a 1ml mixture of polypropylene oxide and accelerated Epon-Araldite (1:1, vol/vol) for 15 minutes. The solution was replaced with 1ml Epon-Araldite and placed in a 60°C oven overnight. Sections were cut at 50 to 100nm, stained with uranyl acetate and lead citrate, and examined with a transmission electron microscope (JEOL, Peabody, MA).

In Vitro Differentiation Assay

The neurospheres were plated on glass slides, pretreated with poly-D-lysine and laminin (or Matrigel, Becton Dickinson) as directed (Cambrex). Differentiation was induced after plating onto an adhesive substrate and removal of mitogens. The cultures were maintained for at least 1 week in Dulbecco's modified eagle medium (GIBCO) with 10% fetal calf serum and 1% penicillin-streptomycin. For analyses of cell types, cell cultures were washed in PBS and fixed with methanol (-80°C) or 4% paraformaldehyde in PBS. Samples were placed in blocking solution with PBS incubated overnight in the appropriate antibody (glial fibrillary acidic protein, microtubule-associated protein 2 [Sigma], and CNPase

[Sternberger Monoclonal, Baltimore, MD]) and processed through standard avidin-biotin amplification (Vectastain) or fluorescent secondaries (CY3 [Jackson Immunoresearch Laboratories] and fluorescein isothiocyanate [Sigma]).¹⁵

Neural Precursor Transplantation

Transplantation procedures and guidelines followed previously published methods.⁹ In brief, cultured MDS and control neural progenitors were labeled independently with rhodamine or fluorescein latex nanospheres (1 μ l/ml; Lumafluor, Naples, FL) over a 24-hour period, washed serially with calcium and magnesium-free Hanks' buffered saline solution, pelleted, and reconstituted to a dilution of 5×10^5 cells/ μ l. Equal volumes of the MDS and control cell suspensions were combined to a final concentration of 1×10^4 cells/ μ l. Cellular transplants were performed on postnatal days 3 through 6 Balb-C mice from our institutional colony. Cell suspensions were slowly pressure injected into the underlying white matter beneath the cortex via a pulled-glass micropipette with tip diameters of approximately 100 μ m. After closing overlying skin, mice were returned to normal care until perfusion for histological analysis.

Statistical Analysis

The distributions of neural progenitor distance from the site of injection were compared using the Kolmogorov–Smirnov two-sample test (nonparametric test assessing differences in distribution). A significant value means two samples have different distributions. The distributions of distance from site of injection were also compared using the Mann–Whitney *U* test (nonparametric test assessing differences in location of ranked data).

In Vitro Proliferation Assay

The proliferation assay follows previously published methods.¹⁴ The human neural precursors are incubated with bromodeoxyuridine (BrdU; 100 μ M) in neurosphere media over a 24- or 48-hour period. Cultures were fixed in 4% paraformaldehyde in PBS, and immunocytochemistry with anti-BrdU (Boehringer Mannheim Biochemicals, Indianapolis, IN) was performed using previously described protocols.¹² Random fields containing individual neurospheres were imaged using a fluorescent Olympus microscope with a SPOT-RT digital camera system or a Zeiss confocal microscope (Harvard Medical School Neurobiology Microscopy Core, Boston, MA). The number of BrdU-positive cells per unit area arising from a single neurosphere was counted using standard imaging software (National Institutes of Health image version 1.62). Comparisons were made between neural progenitors derived from a normal brain and progenitors derived from an MDS brain.

Cell Death Detection

The cell death detection by terminal deoxynucleotidyltransferase-mediated deoxyuridine triphosphate nick end labeling staining followed methods outlined by the manufacturer (In Situ Cell Death Detection kit, TMR red; Roche Diagnostics, Indianapolis, IN). Cultures were fixed with 4% paraformaldehyde in PBS, incubated in labeling solution with enzyme

(9:1, vol/vol) at 37°C, washed, and viewed under rhodamine fluorescence confocal microscopy.

Results

Human neural precursors were isolated from the cerebral wall of a 33-week postmortem fetus with MDS (Fig 1). Clonal populations were obtained from single cells isolated by dissociation from the subventricular zone of the frontal cortex and passage through a cell strainer. By 10 days in vitro, these precursors had expanded and adopted the characteristic floating “neurosphere” morphology and could be subcultured and then reexpanded (see Fig 1A). To exclude potential mosaicism, we performed fluorescent in situ hybridization for the *LIS1* gene with all cells (50/50 cells) demonstrating haploinsufficiency for the gene in metaphase and nondividing interphase (see Fig 1B). Western blot analyses suggested an approximately 50% reduction in *LIS1* protein expression (see Fig 1C), and morphologically these neurospheres appeared undifferentiated by electron microscopy without characteristic neuronal or glial phenotypes (see Fig 1D). These precursors also express neural precursor markers nestin and vimentin (see Figs 1E, F). Microsatellite analysis of the MDS region for loss of heterozygosity showed a typical 3.5Mb deletion, which included the *LIS1* gene. Finally, the neural precursors could differentiate into neurons (microtubule-associated protein 2) and glia (glial fibrillary acidic protein) after withdrawal of mitogens from the culture media. An age-matched control was isolated from the same region and generated in the same manner. Taken in sum, these isolated cell populations shared neural precursor characteristics, were positive for a deletion of the MDS/*LIS1* region in chromosome 17p13.3, and caused classical human lissencephaly.

Classical lissencephaly due to *LIS1* mutations is thought to be a disorder of neuronal motility.¹⁶ Because migration involves actin activation in the cell's leading edge and microtubule-controlled retraction in the rear,¹⁷ we examined the localization of both actin and tubulin in cells derived from primary or secondary clones. Marked perinuclear concentration of α -tubulin was seen in the MDS neural precursors when compared with control cells (Figs 2A–C), but no gross changes were observed in the structure of filamentous actin or the Golgi apparatus, as indicated by immunofluorescence staining with phalloidin and GM-130, respectively. We then examined the migratory capacity of the human precursors after transplantation of human precursors in vivo (see Fig 2D).⁹ By 48 hours after transplantation into host adult murine white matter, the human MDS neural precursors displayed a significant reduction in migration distance from the injection site (mean, 103 μ m) compared with control (mean, 150 μ m; $p < 1.74E-05$, Kolmogorov–Smirnov two-

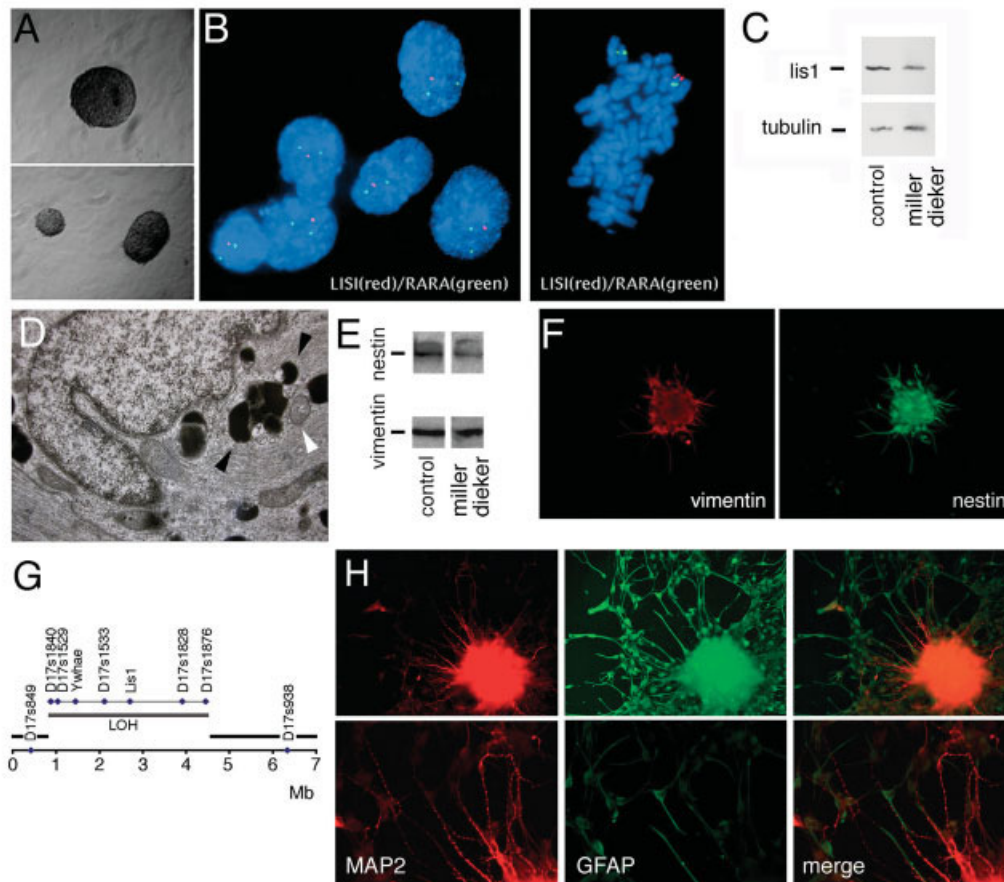


Fig 1. Expansion and characterization of human neural precursors isolated from central nervous system tissue from a Miller-Dieker syndrome (MDS) case, available at postmortem study. (A) Bright-field photomicrograph of neurospheres, derived from the periventricular region of the frontal cortex. (B) Fluorescent in situ hybridization demonstrating loss of an allelic copy of the MDS chromosome 17p13.3 (rhodamine fluorescence) in interphase and after metaphase spread. The control hybridization (fluorescein fluorescence) demonstrates the expected two allelic copies. (C) Western blot showing decreased expression of LIS1 protein in these neural precursors. (D) Electron microscopy demonstrating characteristics of undifferentiated neurospheres including phagocytosed apoptotic bodies (black arrowheads) and prominent lysosomes (white arrowhead). (E) Western blot showing that neural precursors express the early precursor markers nestin and vimentin. (F) Fluorescent photomicrograph showing the typical distribution of these early neural markers within the neurospheres. (G) Microsatellite marker analysis demonstrates loss of heterozygosity (LOH) across a maximal 3.5Mb region corresponding to the MDS deletion and including the LIS1 and YWHAHE genes. (H) One week after culture after removal of growth factors and plating on adhesive substrate, cells can undergo neuronal (rhodamine fluorescence, microtubule-associated protein 2 [MAP2] staining) and glial (fluorescein fluorescence, glial fibrillary acidic protein [GFAP] staining) differentiation. The merged fluorescent photomicrograph shows distinct and nonoverlapping neuronal and glial cell types. Corresponding higher magnification fluorescence photomicrographs (bottom panels) demonstrate extension of long processes and neurite swellings along the processes.

sample test; $p < 9.59E-08$, Mann-Whitney U test). This decreased migratory capacity persisted after 72 hours with MDS compared with control (mean, 150 and 203 μm for MDS and control, respectively; $p < 1.42E-08$, Kolmogorov-Smirnov two-sample test; $p < 1.95E-10$, Mann-Whitney U test). Furthermore, significant differences in migration for both control and MDS neural precursors ($p < 1E-4$ for all comparisons) were observed between the 48- and 72-hour intervals, suggesting that precursors had actively migrated away

from the injection site, but that this migration was deficient in LIS1-deficient human neural stem cells.

Although our transplantation analysis confirmed that a LIS1 deletion causes defects in migration, further analysis of these precursors demonstrated defects in cellular production (Fig 3). Neural precursors were dissociated physically, isolated into individual cells by passage through a filter and dilution, and subsequently allowed to propagate and expand into individual neurospheres. Initial subjective observations suggested that

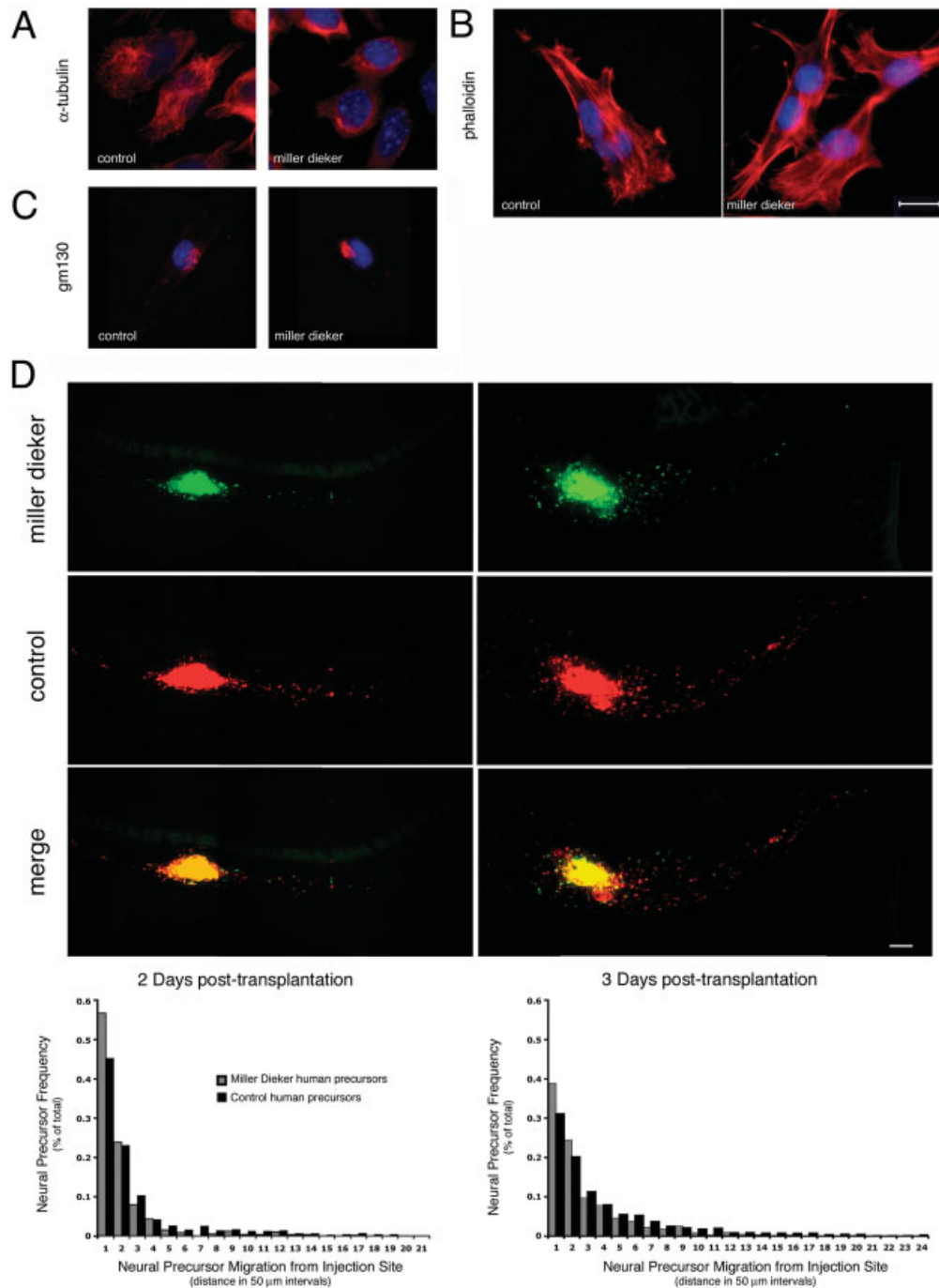


Fig 2. Defect in motility in human Miller-Dieker syndrome (MDS) neural progenitors. (A) Rhodamine fluorescence photomicrographs suggest that disruption of LIS1 leads to abnormal perinuclear expression of α -tubulin, which could disrupt both migration and proliferation. No clear change is seen in (B) microtubule distribution (phalloidin) or (C) Golgi (GM-130) localization. (D) Fluorescence appearance of cotransplanted MDS (fluorescein; gray bars) and normal (rhodamine; black bars) neural progenitors within white matter of mice 2 (left) or 3 (right) days after transplantation. Donor MDS neural precursors do not migrate as far from the injection site as their counterpart normal precursors at both time points. More progenitors have migrated out by 3 days in both cell types. The degree of migration is quantified in the graphs ($n \geq 3$ in each experimental trial; $p < 0.0001$, Kolmogorov-Smirnov two-sample test and Mann-Whitney U test on comparisons between MDS vs control on day 2, MDS vs control on day 3, MDS on day 2 vs MDS on day 3, and control on day 2 vs control on day 3). Scale bar = 100 μ m.

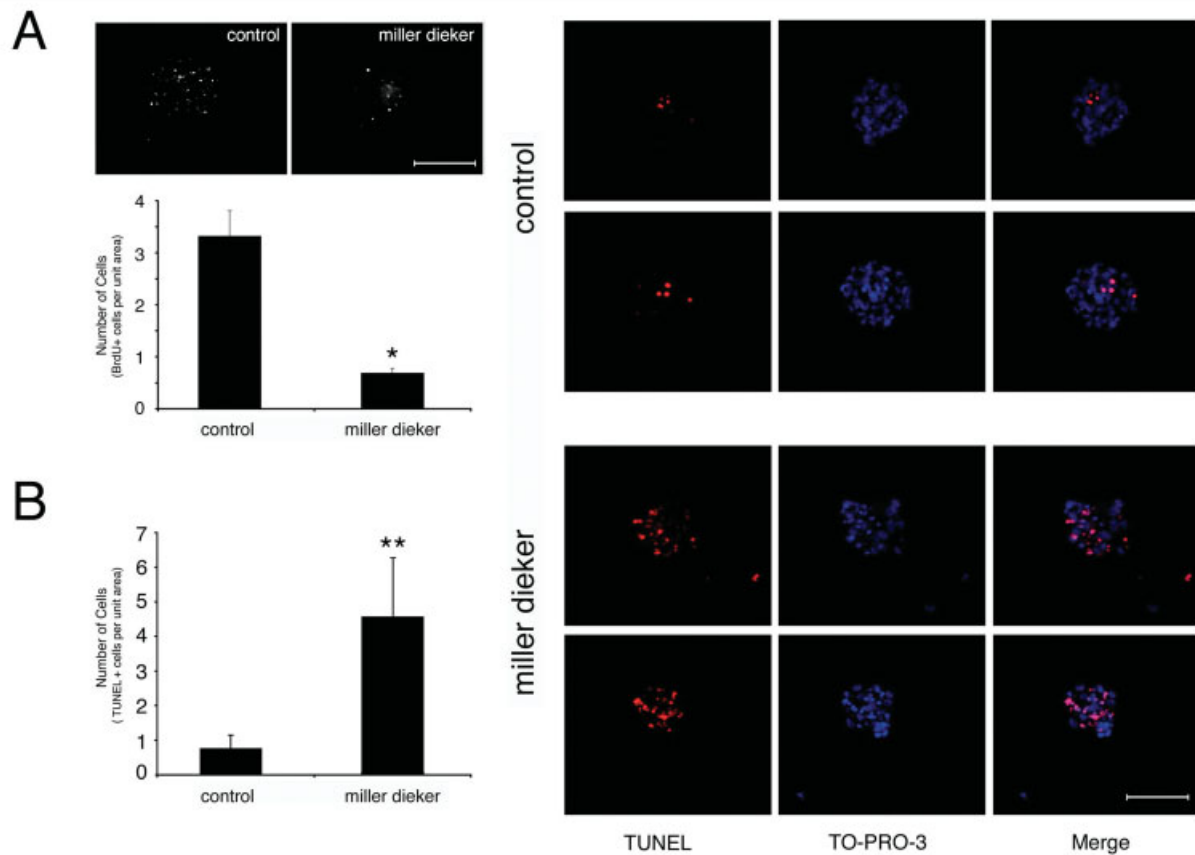


Fig 3. Human Miller-Dieker syndrome (MDS) neural precursors have diminished capacity to proliferate and undergo increased apoptotic cell death. (A) Fluorescence photomicrograph of a typical neurosphere shows decreased uptake of bromodeoxyuridine (BrdU) in human MDS neural precursors compared with control neural precursors. Quantification of BrdU incorporation is shown in the graph below. (B) Fluorescence photomicrograph by confocal microscopy also demonstrates increased numbers of cells undergoing apoptosis as observed by terminal deoxynucleotidyltransferase-mediated deoxyuridine triphosphate nick end labeling (TUNEL) stain in human MDS neural precursors. Quantification of TUNEL-positive cells is shown in the graph to the left. $n \geq 5$ neurospheres in each experimental population; * $p < 0.007$, ** $p < 0.02$ by two-tailed t test. Scale bars = $100\mu\text{m}$.

the MDS neurospheres expanded at a much slower rate. Quantitatively, a reduction of greater than threefold in BrdU incorporation within neurospheres was observed in the MDS neurospheres compared with control over a 24-hour exposure period. The diminished proliferation was due, in part, to increased programmed cell death, as determined by terminal deoxynucleotidyltransferase-mediated deoxyuridine triphosphate nick end labeling staining of the neurospheres, with a more than fourfold increase in the number of apoptotic nuclei. This increase in cell death within the MDS neural precursors, however, likely did not account entirely for the diminished rate of proliferation, because the rate of BrdU incorporation for viable cells alone was still greater in control compared with MDS neural cells (35.3 vs 10.4%).

Discussion

Our analysis of human neural progenitors from a single MDS brain potentially provides several novel insights

into the underlying cause of lissencephaly. From current human and prior animal studies, heterozygous disruption of LIS1 function impairs neuronal migration and motility in a cell autonomous fashion. In MDS, however, the more severe lissencephaly is, in part, also due to impairments in cellular proliferation and increased cell death. These observations suggest a gradient of severity of lissencephaly ranging from the severe lissencephaly in MDS deletions, milder lissencephaly in isolated LIS1 or Doublecortin (*DCX*) mutations, to the mildest lissencephaly with cerebellar hypoplasia in Reelin (*RELN*) mutations. Moreover, our data suggest that the most severe cases of lissencephaly involve defects in earlier developmental stages (proliferation) that could influence later stages of neuronal migration (*LIS1* and *DCX*)^{3,18} and arrest (*RELN*).¹⁹

Interactions among LIS1, 14-3-3 ϵ (encoded by *YWHAE*), and/or other proteins may underlie the proliferative defects within MDS neural precursors and contribute to the severity of this cortical malformation.

Prior reports have already shown a role for Lis1 in proliferation where Lis1 overexpression in mammalian cells leads to interference with mitotic progression and spindle misorientation, whereas injection of anti-lis1 antibody interferes with attachment of chromosomes to the metaphase plate and leads to chromosome loss.^{5,20} Similarly, Lis1 interacts with Nde1 and Ndel1, centrosomal proteins that are involved in the dynamic reorganization of the microtubule organizing center during cell division,^{21–23} and recent findings suggest that *Nde1* null mice demonstrate striking defects in progenitor proliferation and mitotic progression.²⁴ Lis1 effects, however, are dosage dependent, and proliferative defects are not readily apparent in the heterozygous *Lis1* mice^{7,8}; therefore, it could be argued that heterozygous *LIS1* human deletions alone may not be sufficient to produce this abnormality. Rather, it has been suggested that the *Ywhae* gene encoding for 14-3-3 ϵ , one member in a family of ubiquitous phosphoserine/threonine-binding proteins, is always deleted in MDS.¹ The 14-3-3 ϵ protein binds to Ndel1, and inhibition of this protein results in mislocalization of both Ndel1 and Lis1. Thus, combinatorial genetic effects resulting from deletion of *LIS1* and *YWHAE* may cause the worsened MDS phenotype through defects in proliferation. Lastly, the fetus had a small duplication of 1p36. Although this chromosomal abnormality has not been reported to cause congenital microcephaly or other central nervous system features aside from mild developmental delay,²⁵ part of the central nervous system phenotype seen in the progenitor cells could result from this chromosomal abnormality. That said, all of the characteristic brain features seen in this case study can be attributed to the known features seen with MDS and chromosome 17p deletions.

Because inherited human disorders of proliferation typically cause microcephaly (small brain) with preservation of sulci and gyri, the combination of microcephaly plus the worsened lissencephaly seen in MDS must reflect multiple abnormal processes.²⁶ Changes in cell cycle timing through impaired proliferation may alter the precise sequence of neuronal migration. M-phase prolongation has been observed with Lis1 overexpression and Nde1 inhibition in culture.^{5,24} Our histological examination of MDS tissue suggests that a greater proportion of proliferative cells are aligned along the disrupted ventricular ependymal lining, where proliferative cells in M-phase cells typically reside.²⁷ In addition, as has been suggested elsewhere and appreciated in this study, a band of later born neurons resides in the deepest layer 4 of the MDS cortex and underneath the relatively normal lamination of the MDS cortex.^{27,28} Defects in cell motility due to heterozygous *Lis1* mutations have been shown to cause a preferential impairment in migration of later born neurons,⁸ but cell-cycle prolongation with delayed exit of later born

neurons from the cell cycle could also disrupt the capacity of these neurons to migrate out of the ventricular zone into the cortical plate. Thus, changes in cell number and timing can contribute to the severity of lissencephalic brain.

By showing differences in the functional behavior between human neural stem cells with an MDS deletion and mouse cells, our work suggests the importance of human neural precursor cell lines for studying genetic diseases. The capacity to isolate, expand, and then study the functional aspects of human neural cells derived from a variety of central nervous system developmental disorders will now provide a means to approach the mechanistic processes that cause these diseases, especially in the setting where animal models are neither sufficient nor satisfactory.

This work was supported by the NIH (National Institute of Neurological Disorders and Stroke, 2R37 NS35129 and 1P01NS40043, C.A.W.; National Institute of Mental Health, 1K08MH/NS63886-01, V.L.S.), the March of Dimes (C.A.W.), the McKnight Foundation (C.A.W.), the Howard Hughes Medical Institute (C.A.W.), Julian and Carol Cohen (V.L.S.), the Ellison Foundation (V.L.S.), the Milton Fund, (V.L.S.), a Charles A. Dana Fellowship (V.L.S.), a Beckman Young Investigator (V.L.S.), and the Leukaemia Research Fund (A.H.B., P.J.B.).

References

1. Toyo-oka K, Shionoya A, Gambello MJ, et al. 14-3-3epsilon is important for neuronal migration by binding to NUDEL: a molecular explanation for Miller-Dieker syndrome. *Nat Genet* 2003;34:274–285.
2. Mizuguchi M, Takashima S, Kakita A, et al. Lissencephaly gene product. Localization in the central nervous system and loss of immunoreactivity in Miller-Dieker syndrome. *Am J Pathol* 1995;147:1142–1151.
3. Reiner O, Carrozzo R, Shen Y, et al. Isolation of a Miller-Dieker lissencephaly gene containing G protein beta-subunit-like repeats. *Nature* 1993;364:717–721.
4. Lo Nigro C, Chong CS, Smith AC, et al. Point mutations and an intragenic deletion in *LIS1*, the lissencephaly causative gene in isolated lissencephaly sequence and Miller-Dieker syndrome. *Hum Mol Genet* 1997;6:157–164.
5. Faulkner NE, Dujardin DL, Tai CY, et al. A role for the lissencephaly gene *LIS1* in mitosis and cytoplasmic dynein function. *Nat Cell Biol* 2000;2:784–791.
6. Smith DS, Niethammer M, Ayala R, et al. Regulation of cytoplasmic dynein behaviour and microtubule organization by mammalian Lis1. *Nat Cell Biol* 2000;2:767–775.
7. Hirotsune S, Fleck MW, Gambello MJ, et al. Graded reduction of Pafah1b1 (*Lis1*) activity results in neuronal migration defects and early embryonic lethality. *Nat Genet* 1998;19:333–339.
8. Gambello MJ, Darling DL, Yingling J, et al. Multiple dose-dependent effects of *Lis1* on cerebral cortical development. *J Neurosci* 2003;23:1719–1729.
9. Sheen VL, Macklis JD. Targeted neocortical cell death in adult mice guides migration and differentiation of transplanted embryonic neurons. *J Neurosci* 1995;15:8378–8392.
10. Bahn S, Mimmack M, Ryan M, et al. Neuronal target genes of the neuron-restrictive silencer factor in neurospheres derived from fetuses with Down's syndrome: a gene expression study. *Lancet* 2002;359:310–315.

11. Sheen VL, Wheless JW, Bodell A, et al. Periventricular heterotopia associated with chromosome 5p anomalies. *Neurology* 2003;60:1033–1036.
12. Sheen VL, Arnold MW, Wang Y, Macklis JD. Neural precursor differentiation following transplantation into neocortex is dependent on intrinsic developmental state and receptor competence. *Exp Neurol* 1999;158:47–62.
13. Sheen VL, Macklis JD. Apoptotic mechanisms in targeted neuronal cell death by chromophore-activated photolysis. *Exp Neurol* 1994;130:67–81.
14. Sheen VL, Ganesh VS, Topcu M, et al. Mutations in ARF-GEF2 implicate vesicle trafficking in neural progenitor proliferation and migration in the human cerebral cortex. *Nat Genet* 2004;36:69–76.
15. Sheen VL, Feng Y, Graham D, et al. Filamin A and Filamin B are co-expressed within neurons during periods of neuronal migration and can physically interact. *Hum Mol Genet* 2002;11:2845–2854.
16. Wynshaw-Boris A, Gambello MJ. LIS1 and dynein motor function in neuronal migration and development. *Genes Dev* 2001;15:639–651.
17. Wehrle-Haller B, Imhof BA. Actin, microtubules and focal adhesion dynamics during cell migration. *Int J Biochem Cell Biol* 2003;35:39–50.
18. Gleeson JG, Allen KM, Fox JW, et al. Doublecortin, a brain-specific gene mutated in human X-linked lissencephaly and double cortex syndrome, encodes a putative signaling protein. *Cell* 1998;92:63–72.
19. Hong SE, Shugart YY, Huang DT, et al. Autosomal recessive lissencephaly with cerebellar hypoplasia is associated with human RELN mutations. *Nat Genet* 2000;26:93–96.
20. Vallee RB, Faulkner NE, Tai CY. The role of cytoplasmic dynein in the human brain developmental disease lissencephaly. *Biochim Biophys Acta* 2000;1496:89–98.
21. Feng Y, Olson EC, Stukenberg PT, et al. LIS1 regulates CNS lamination by interacting with mNudE, a central component of the centrosome. *Neuron* 2000;28:665–679.
22. Niethammer M, Smith DS, Ayala R, et al. NUDEL is a novel Cdk5 substrate that associates with LIS1 and cytoplasmic dynein. *Neuron* 2000;28:697–711.
23. Sasaki S, Shionoya A, Ishida M, et al. A LIS1/NUDEL/cytoplasmic dynein heavy chain complex in the developing and adult nervous system. *Neuron* 2000;28:681–696.
24. Feng Y, Walsh CA. Mitotic spindle regulation by Nde1 controls cerebral cortical size. *Neuron* 2004;44:279–293.
25. Heilstedt HA, Shapira SK, Gregg AR, Shaffer LG. Molecular and clinical characterization of a patient with duplication of 1p36.3 and metopic synostosis. *Clin Genet* 1999;56:123–128.
26. Sheen VL, Walsh CA. Developmental genetic malformations of the cerebral cortex. *Curr Neurol Neurosci Rep* 2003;3:433–441.
27. Sheen V, Ferland R, Neal J, et al. Neocortical Neuronal Arrangement in Miller Dieker Syndrome. *Acta Neuropathol (Berl)* 2006; Feb 3:1–8.
28. Caviness VS Jr. Mechanical model of brain convolitional development. *Science* 1975;189:18–21.